Field-induced-magnetic-moment form factor of metallic chromium

C. Stassis, G. R. Kline, and S. K. Sinha
Ames Laboratory–USAEC and Department of Physics, Iowa State University, Ames, Iowa 50010
(Received 15 August 1974)

Polarized-neutron techniques have been used to study the spatial distribution and temperature dependence of the field-induced magnetic moment in metallic chromium. It is demonstrated that the coherent magnetic scattering of neutrons by the induced magnetic moment in chromium may be described in terms of free-ion form factors. The angular distribution of the magnetic scattering is best fitted by having a 60% $3d$ orbital-40% $3d$ spin contribution to the induced moment both above and below the antiferromagnetic transition temperature of the sample. The orbital and spin contribution to the static susceptibility were found to be $(98 \pm 3) \times 10^{-6}$ emu/mol and $(65 \pm 2) \times 10^{-6}$ emu/mol, respectively; the gyromagnetic ratio is 1.25 ± 0.04. These results are in good agreement with bulk-susceptibility measurements performed on the same sample, as well as with independent measurements of the gyromagnetic ratio of chromium. The magnitude of the localized induced moment has been found to be temperature independent in the (27–200) °C temperature region. This result implies the absence of any well-defined local moment above the antiferromagnetic transition temperature of the sample.

I. INTRODUCTION

Since the first demonstration by Shull and Wilkinson[1] that metallic chromium is antiferromagnetic, there have been a considerable number of investigations towards an understanding of its properties. Presently, it is generally accepted that chromium is an itinerant electron antiferromagnet, whose electronic properties are associated with spin-density waves of the type first discussed by Overhauser.[2] The itinerant model has not been solved exactly, but the mean-field theory seems to account for most of the observed phenomena.

One of the predictions of the mean-field theory is that there are no local magnetic moments above the Néel temperature (~40 °C), and that magnetic moments form on the atoms only when the metal is in the antiferromagnetic state. Neutron paramagnetic scattering experiments[3] clearly demonstrated the absence of any local moments at 210 °C. On the other hand NMR measurements,[4] in the (40–100) °C temperature region, have been interpreted in terms of well-defined local moments. The spatial distribution of the magnetization is also of particular interest, since Cr is an itinerant-electron metal. In the ordered state, the spatial distribution of the magnetization has been determined by Moon, Koehler, and Trego[5] from the intensities of the antiferromagnetic reflections of Cr. They found that the magnetic form factor is in good agreement with a $3d$-spin atomic form factor. In the present investigation polarized-neutron techniques have been used to study the spatial distribution and temperature dependence of the magnetization induced in metallic chromium by an externally applied magnetic field.

In the polarized-neutron technique, the induced magnetic moment is sensed through the interference of its neutron magnetic scattering with the nuclear scattering. The quantity determined by the measurements is the *coherent* paramagnetic scattering amplitude. Since the measurements are performed at the Bragg reflections of the crystal, the spatial distribution and temperature dependence of the induced moment may be studied below as well as above the antiferromagnetic transition temperature. The angular dependence of the coherent paramagnetic scattering amplitude can, in principle, establish (a) whether the spatial distribution of the induced moment is appreciably different from that of a free ion, in view of the fact that chromium is a typical itinerant-electron metal, and (b) the electronic character of the field-induced magnetization and its distribution between orbital and electron spin polarization. Only the nonuniform magnetization induced within a few angstroms of a lattice site is sensed at the Bragg reflections of the crystal. Therefore, the presence of a well-defined localized spin above the Néel point will manifest itself in the temperature dependence of the coherent paramagnetic scattering amplitude.

Preliminary measurements of the present investigation have been reported in an earlier communication.[6] In the present paper we give a complete account of these experiments.

II. COHERENT PARAMAGNETIC SCATTERING AMPLITUDE

In metallic chromium there is experimental evidence[5] that the orbital moment is quenched by the crystalline field and that the spin-orbit interaction does not introduce any significant admixture of higher orbital moment states into the ground

state. However, in the presence of an external magnetic field, in addition to the induced spin moment, an orbital moment will be induced[7] as a result of the admixture by the magnetic field of higher orbital moment states into the ground state. The induced orbital moment is expected to be significant, since the Fermi level of chromium lies between two peaks, of predominately d-like character, in the density of states. Thus the induced moment paramagnetic scattering amplitude will consist of a spin and an orbital scattering term.

The induced-moment paramagnetic scattering amplitude $p(\theta)$ is proportional to the Fourier transform $M_z(\vec{q})$ of the induced magnetic moment in the crystal

$$p(\theta) = (\mu_n r_0)(1/2\mu_B) M_z(\vec{q}). \tag{1}$$

In Eq. (1), $\mu_n = 1.91$ is the magnetic moment of the neutron in nuclear magnetons, r_0 is the classical electron radius, $\vec{q}$ is the neutron scattering vector of magnitude $4\pi \sin\theta/\lambda$, λ is the wavelength, and 2θ denotes the scattering angle. In writing Eq. (1), the z axis was chosen to coincide with the direction of the external magnetic field. In the absence of significant spin-orbit coupling the induced magnetization consists of a spin and an orbital component. Linear response theory shows[8] that the Fourier transform of the induced magnetic moment can be expressed in terms of the off diagonal components of the static generalized susceptibility function

$$M_z(\vec{q}) = [\chi^{zz}_{\text{orb}}(\vec{q}, \vec{q}') + \chi^{zz}_{\text{spin}}(\vec{q}, \vec{q}')] H_z(\vec{q}'), \tag{2}$$

where the applied magnetic field is given by

$$\vec{H}(\vec{r}) = \hat{z} H_z(\vec{q}')\, e^{i\vec{q}'\cdot\vec{r}}. \tag{3}$$

Under the conditions of the present experiment $\vec{q}' \to 0$ and the induced moment paramagnetic scattering amplitude can be written

$$p(\theta) = (\mu_n r_0)(H/2\mu_B)[\chi^{zz}_{\text{orb}}(\vec{q}, 0) + \chi^{zz}_{\text{spin}}(\vec{q}, 0)], \tag{4}$$

where H is the magnitude of the static magnetic field applied to the crystal. Thus a measurement of the induced moment paramagnetic scattering amplitude provides directly the $\vec{q}$ dependence of the component $\chi^{zz}(\vec{q}, 0)$ of the susceptibility function.

In the absence of exchange interactions the spin part of the susceptibility function may be written

$$\chi^{zz}_{\text{spin}}(\vec{q}, \vec{q}') = -\mu_B^2 \sum_{\substack{k,k' \\ \sigma}} \frac{n_{k\sigma} - n_{k'\sigma}}{E_{k\sigma} - E_{k'\sigma}} \times \langle \psi_{k\sigma} | e^{-i\vec{q}\cdot\vec{r}} | \psi_{k'\sigma} \rangle \langle \psi_{k'\sigma} | e^{i\vec{q}'\cdot\vec{r}} | \psi_{k\sigma} \rangle, \tag{5}$$

where k, k' denote the electronic wave vectors, σ is a spin index, $\psi_{k\sigma}$ and $\psi_{k'\sigma}$ denote Bloch wave functions with energy eigenvalues $E_{k\sigma}$ and $E_{k'\sigma}$, respectively, and $n_{k\sigma}$, $n_{k'\sigma}$ are occupation numbers. In a crystal, $\vec{q} - \vec{q}'$ must be a reciprocal-lattice vector. Thus as $\vec{q}' \to 0$, $\vec{q}$ must tend to a reciprocal-lattice vector. Therefore, the coherent paramagnetic scattering amplitude measured in the present experiment is given by Eq. (4) where $\vec{q}$ is a reciprocal-lattice vector. The matrix element of $e^{i\vec{q}'\cdot\vec{r}}$ appearing in Eq. (5) tends to unity, as $\vec{q}' \to 0$, for intraband transitions and it vanishes for interband transitions; furthermore this matrix element is zero if $k' \neq k$. Thus Eq. (5) reduces to

$$\chi^{zz}_{\text{spin}}(\vec{q}, \vec{q}' \to 0) = \mu_B^2 \sum_{k\sigma} \frac{1}{|\nabla_k E_{k\sigma}|} \times \langle \psi_{k\sigma} | e^{-i\vec{q}\cdot\vec{r}} | \psi_{k\sigma} \rangle, \tag{6}$$

where the sum is only over states at the Fermi level. The right-hand side of Eq. (6) is, as expected, a density-of-states weighted form factor for states at the Fermi level. If we make the approximation that the right-hand side of Eq. (5) can be factorized into a $\vec{q}$ and $\vec{q}'$ part, then it can be shown[8] that the exchange enhancement simply multiplies the above expression by a factor which is periodic in reciprocal space. With this assumption the $\vec{q}$ dependence of the spin part of the coherent paramagnetic scattering amplitude is given by Eq. (6). If the states $\psi_{k\sigma}$ may be expressed as combinations of tight-binding d-orbitals and a few orthogonalized plane waves then Eq. (6) shows that the main contribution to the form factor is from states of mainly d-like character, because such states contribute predominantly to the density of states at the Fermi level. In this case we may neglect the orthogonalized-plane-wave (OPW) components of the wave functions. If in addition, we neglect overlapping of the d functions, the spin part of the paramagnetic scattering amplitude may be written

$$[p(\vec{q})]_{\text{spin}} = \tfrac{1}{2}(\mu_n r_0) H a n_d(E_F) \langle \varphi_d | e^{-i\vec{q}\cdot\vec{r}} | \varphi_d \rangle, \tag{7}$$

where a is the exchange enhancement factor, $n_d(E_F)$ is the density of d states at the Fermi level, and $|\varphi_d\rangle$ is a tight-binding d orbital. Equation (7) is in a convenient form for band theoretical calculations of the form factor. However, if the assumptions leading to Eq. (7) are valid than a good approximation for the form factor can be obtained using ionic wave functions. In fact the latter form factor is not substantially different from the spin form factor obtained by band theoretical calculations.[9]

The calculation of $\chi^{zz}_{\rm orb}(\vec{q}, 0)$ in terms of Bloch wave functions is a difficult computational problem. However, it may be shown that apart from terms that vanish in the limit of tight binding

$$\chi^{zz}_{\rm orb}(\vec{q}, 0) = \left(\frac{ir_0}{2q}\right) \sum_{k,\lambda,\lambda',\sigma} \frac{n_{k\sigma,\lambda}(1-n_{k\sigma,\lambda})}{E_{k\sigma,\lambda}-E_{k\sigma,\lambda'}} \times \langle \psi_{k\sigma,\lambda} | Q_z(\vec{q}) | \psi_{k\sigma,\lambda'} \rangle_0 \times \langle \psi_{k\sigma,\lambda} | L_z | \psi_{k\sigma,\lambda} \rangle_0 . \quad (8)$$

in Eq. (8) the Bloch wave-vector index k and the band indices λ, λ' have been introduced explicitly, L_z is the z component of the angular momentum operator, Q_z is the z component of the operator

$$\vec{Q} = (1/2m)\hat{q} \times (\vec{p} e^{i\vec{q}\cdot\vec{r}} + e^{i\vec{q}\cdot\vec{r}} \vec{p}), \quad (9)$$

m is the electronic mass, $\vec{p}$ denotes the momentum of an electron, and $\hat{q}$ is the unit scattering vector $\vec{q}/|\vec{q}|$. Equation (8) is a generalization of the Kubo-Obata[7] expression for the static orbital susceptibility. The diamagnetic contribution to the orbital part of the susceptibility function is not included in Eq. (8) but can be taken into account in the analysis of the experimental data. The form factor given by Eq. (8) cannot be further simplified without reference to the particular band structure of the metal. An examination of the electronic energy band structure of paramagnetic chromium shows that the d bands separate into two distinct groups, which apart from hybridization and band broadening effects, may be thought of as a crystal-field splitting of ionic d states into a t_{2g} triplet and a higher lying e_g doublet. To obtain an approximate expression, we assume that we have a completely filled set of t_{2g} levels and an unfilled set of e_g levels. In this case Eq. (8) can be written

$$\chi^{zz}_{\rm orb}(\vec{q}, 0) = \left(\frac{ir_0}{2q}\right) \sum_{\alpha,\beta} \frac{1}{\Delta} \langle t^{\alpha}_{2g} | Q_z | e^{\beta}_g \rangle \times \langle e^{\beta}_g | L_z | t^{\alpha}_{2g} \rangle , \quad (10)$$

where Δ represents the mean separation of the two subbands and α and β label the states in the t_{2g} and e_g representations, respectively. In general the magnitude and the q dependence of $\chi^{zz}_{\rm orb}(q, 0)$ depend on the direction of the applied magnetic field relative to the crystallographic axes. However, in the present experiment, measurements of the magnetic scattering amplitude of the (110) reflection with the field applied along the [001], [1$\bar{1}$0], and [1$\bar{1}$1] directions were found to agree, to within experimental precision. Therefore the calculation of the orbital form factor can be performed by taking the magnetic field along the [001] direction. Denoting the atomic d functions by $|2m\rangle$, these states may be written $|t^1_{2g}\rangle = |2,1\rangle$, $|t^2_{2g}\rangle = |2,-1\rangle$, $|t^3_{2g}\rangle = (1/\sqrt{2})(|2,2\rangle - |2,-2\rangle)$, $|e^1_g\rangle = |2,0\rangle$, and $|e^2_g\rangle = (1/\sqrt{2})(|2,2\rangle + |2,-2\rangle)$. The L_z matrix element in Eq. (10) allows only transitions between the $|t^3_{2g}\rangle$ and $|e^2_g\rangle$ states. In addition, the only nonzero matrix elements of the operator Q_z are $\langle 2,2|Q_z|2,2\rangle$ and $\langle 2,-2|Q_z|2,-2\rangle$. Taking into account that these matrix elements are equal and of opposite sign one obtains

$$\chi^{zz}_{\rm orb}(\vec{q}, 0) = \frac{e^2}{2mc^2} \frac{i}{q} \frac{1}{\Delta} \langle 2,2|Q_z|2,2\rangle . \quad (11)$$

It is interesting to note that for $\vec{q}$ perpendicular to the z axis, the direction of the external magnetic field, the orbital form factor is isotropic. Thus, within the assumptions of this simple model, the anisotropy of the induced moment form factor must arise only from the spin part of the scattering amplitude.

III. EXPERIMENTAL

In the present experiment a polarized monochromatic neutron beam is incident on the crystal oriented for Bragg reflection and subjected to an external magnetic field normal to the scattering plane. The quantity measured is the polarization ratio R defined as the ratio of the coherent diffracted intensities for the two-neutron spin orientations, parallel and antiparallel to the applied field, respectively. The coherent paramagnetic scattering amplitude $p(\theta)$ is simply related to the measured residual polarization ratio r_m defined as $r_m = R - 1$. Under the conditions of the present experiment the measured residual polarization ratio may be written

$$r_m = r_c + r_d + r_{\rm so} , \quad (12)$$

where

$$r_c = 4p(\theta)/b , \quad (13)$$

$$r_d = -\frac{2\mu_n Z r_0}{b} \left(\frac{eH}{\hbar c}\right) \frac{1}{q} \frac{df_a(q)}{dq} , \quad (14)$$

$$r_{\rm so} = \frac{4b'\gamma \cot\theta}{b^2} . \quad (15)$$

In Eq. (12), the second term[10] arises from the interaction of the magnetic moment of the neutron with the field-induced diamagnetic moment and the third term is due to the neutron-spin–neutron-orbit interaction[11] in the Coulomb field of the atom. Equations (14) and (15), for the diamagnetic and spin-orbit terms, are strictly valid for a free ion. They are not expected to be significantly different in the solid and will be adopted in the present analysis. In writing these equations, it has been assumed that the neutron spin dependent part of the scattering amplitude is small in comparison with

the coherent nuclear scattering amplitude b, a condition fulfilled in our measurements. In Eq. (14), Z is the atomic number and $f_a(q)$ is the atomic charge form factor. In Eq. (15),

$$\gamma = \tfrac{1}{2}\mu_n Z(e^2/Mc^2)[1 - f_a(q)], \tag{16}$$

where M is the neutron mass, and b' is the imaginary part of the nuclear scattering amplitude. Both the diamagnetic and spin-orbit contributions to the coherent scattering amplitude of Cr are small in comparison with the paramagnetic contribution. In the most severe case of the (110) reflection, the diamagnetic and spin-orbit contribution amount to approximately 8 and 4% of the measured residual polarization ratio respectively. Thus, the experimental data, after corrections for the diamagnetic and spin-orbit contribution, provide a measurement of the paramagnetic scattering amplitude $p(\theta)$, which can be compared with theoretical calculations.

In a magnetic field of 22 kOe, the residual polarization ratios range from a few parts per 10 000 to a few parts per 1000. In order to measure these small residual polarization ratios in a reasonable time, the diffracted beam intensity must be of the order of a few thousand neutrons per second. For the available neutron flux, intensities of this magnitude may be obtained only by using single crystals. The single crystals used in the present experiment have been grown by the arc zone melting technique[12] using high-purity chromium.

The polarization ratios that one measures using single crystals must be corrected for secondary extinction effects. To minimize the size of this correction, the sample used consisted of three 2-mm-thick slices cemented together with Duco cement. The mosaic spread of the three crystal slices was gradually increased by successive compressions, until integrated reflectivity measurements indicated that the composite-slice sample was practically free of extinction.

The measurements were performed in the (27–200) °C temperature region with the sample mounted in a high-vacuum furnace. The temperature of the sample was measured by a thermocouple, and it was controlled to within 0.5 °C by a controller operated through a second thermocouple incorporated in the sample holder. The measurements, with a 22.2 kOe magnetic field on the sample, were performed using a highly polarized neutron beam at the 5-MW Ames Laboratory Research Reactor. The neutron wavelength λ was 1.05 Å with a $\frac{1}{2}\lambda$ contamination of approximately 0.6%. In measuring small polarization ratios, the drifting of the diffraction peak intensity can introduce a sizable correction. To avoid this problem the neutron spin was flipped twenty times per second and the scattered neutrons of the two spin states were counted in two separate scalars. In order to assess the presence of any hysteresis effects, the polarization ratios of several reflections were measured on cooling as well as warming of the crystal. The measured polarization ratios were found to agree to within experimental precision.

IV. EXPERIMENTAL RESULTS AND DISCUSSION

The angular dependence of the paramagnetic scattering amplitude was measured below as well as above the 40 °C antiferromagnetic transition temperature of the sample. The room-temperature form factor was obtained by measuring the polarization ratios of the (110), (200), (211), (220), (321), (330), and (411) reflections. The angular dependence of the paramagnetic scattering amplitude, at 100 °C, was obtained by measuring the polarization ratios for the (110), (200), (211), (220), and (310) reflections. The measured residual polarization ratios r_m, corrected for background, are tabulated in Table I. The induced moment scattering amplitude is obtained after correction of the measured polarization ratio for the diamagnetic and spin-orbit contribution

$$r_c \equiv 4p(\theta)/b = r_m - r_d - r_{so}\,. \tag{17}$$

The diamagnetic and spin-orbit corrections have been calculated using the formulae of Sec. II and are listed together with r_c in Table I. It is seen (Table I) that the polarization ratios at 100 °C agree, to within experimental precision, with those at room temperature. This implies that the spatial distribution of the induced moment does not change appreciably as the temperature is increased above 40 °C, the antiferromagnetic transition temperature of the sample.

The angular dependence of the paramagnetic scattering amplitude is compared with the magnetic form factor of the ordered state in Fig. 1. The magnetic form factor of the ordered state has been determined by Moon, Koehler, and Trego[5] from the intensities of the antiferromagnetic reflections of Cr. Our data have been normalized to a forward scattering amplitude corresponding to a static susceptibility of 160×10^{-6} emu/mol, as determined for our sample[13] by the Faraday method. The induced moment form factor decreases less rapidly with increasing angle than the magnetic form factor of the ordered state. This implies that the induced moment density distribution is less extended in space than the spin density in the ordered state. This suggests that a large part of the induced moment is of orbital origin.

A detailed comparison of the experimental data with theoretical calculations is not presently possible, since band theoretical calculations of the

TABLE I. Measured and corrected residual-polarization ratios for some reflections of Cr. The magnetic field on the crystal is 22 200 Oe. For chromium, $b = 0.3532 \times 10^{-12}$ cm and for $\lambda = 1.05$ Å, $b' = 3.72 \times 10^{-16}$ cm.

Reflections	$T = 27\,^{\circ}C$ $10^4 r_m$	$T = 100\,^{\circ}C$ $10^4 r_m$	$10^4 r_d$	$10^4 r_{so}$	$T = 27\,^{\circ}C$ $10^4 r_c$	$T = 100\,^{\circ}C$ $10^4 r_c$
(110)	11.31 ± 0.46	10.93 ± 0.23	−0.899	0.472	11.73 ± 0.47	11.36 ± 0.24
(200)	7.40 ± 0.60	7.55 ± 0.26	−0.527	0.461	7.46 ± 0.61	7.61 ± 0.27
(211)	5.91 ± 0.48	5.90 ± 0.33	−0.348	0.432	5.82 ± 0.49	5.82 ± 0.35
(220)	4.40 ± 0.43	4.34 ± 0.36	−0.240	0.398	4.24 ± 0.43	4.18 ± 0.38
(310)	•••	3.26 ± 0.43	−0.166	0.361	•••	3.06 ± 0.45
(321)	2.42 ± 0.64	•••	−0.097	0.256	2.26 ± 0.65	•••
(330)	1.42 ± 0.74	•••	−0.062	0.237	1.24 ± 0.75	•••
(411)	0.83 ± 0.78	•••	−0.062	0.237	0.65 ± 0.80	•••

induced-spin and -orbital form factors of chromium are not available. However, there is abundant evidence in other transition metals that atomic form factors provide in most cases an excellent description of the magnetic scattering. In addition, the magnetic-spin form factor of chromium in the ordered state, calculated by band theory,[14] is essentially identical with the free atom spin form factor. Both the free-atom spin form factor and the band theoretical ordered spin form factor are in excellent agreement with the experimental results of Moon *et al.*[5] In order to see whether the induced-moment form factor could also be interpreted in terms of free-atom factors, the experimental data were fitted with form factors obtained by assuming ionic wave functions. The spin form factor [Eq. (7)] is simply an ionic form factor, and the orbital form factor can be calculated from Eq. (11) by well-known techniques.[15] In these calculations the ionic radial integrals of Freeman and Watson[16] have been used. The data are best fitted by having a 60% $3d$ orbital–40% $3d$ spin contribution to the induced moment (Fig. 2). The zero-angle residual-polarization ratio, obtained by extrapolation, is 19.9 ± 0.6 and corresponds to a static susceptibility of $(163 \pm 5) \times 10^{-6}$ emu/mol. This value is to be compared with a total susceptibility of 160×10^{-6} emu/mol measured by the Faraday method on the same sample.[13] The close agreement between the $3d$ susceptibility obtained from the neutron diffraction data and the total susceptibility implies that the $4s$ electron contribution to the total susceptibility is small and comparable in magnitude with the chromium diamagnetism. The $3d$ spin and orbital susceptibilities obtained from the analysis of the neutron diffraction data, are $(65 \pm 2) \times 10^{-6}$ emu/mol and $(98 \pm 3) \times 10^{-6}$ emu/mol, respectively. The large orbital contribution to the susceptibility implies that the gyromagnetic ratio g for chromium must be appreciably smaller than 2. In fact from our measurements $g = 1.25 \pm 0.04$. This is in excellent agreement with the value 1.21 ± 0.07 obtained in a direct measurement[17] of the gyromagnetic ratio of chromium by the Einstein–de Haas method. Since the polarization ratios of the (330) and (411) reflections (that occur at the same value of $\sin\theta/\lambda$) differ by less than a standard deviation, no definite conclusion may be drawn regarding the departure from spherical symmetry of the induced moment distribution around a lattice point. However, the observed difference may be accounted for by assuming that the anisotropy arises entirely from the spin part of the susceptibility function and that the induced spin distribution is predominately of t_{2g} character. In fact under these assumptions the calculated $4p(\theta)/b$ value for the (330) and (411) reflections are 1.41 and 0.85, respectively.

The temperature dependence of the paramagnetic scattering amplitude, in the (27–200) °C temperature region, has been obtained by measuring the polarization ratio of the (110) Bragg reflection. The data are summarized in the insert of Fig. 2. It is seen that the magnetic scattering amplitude is essentially temperature independent. Thus, to within experimental precision, we do not observe the temperature dependence expected for an intrinsic localized spin on the chromium atoms.

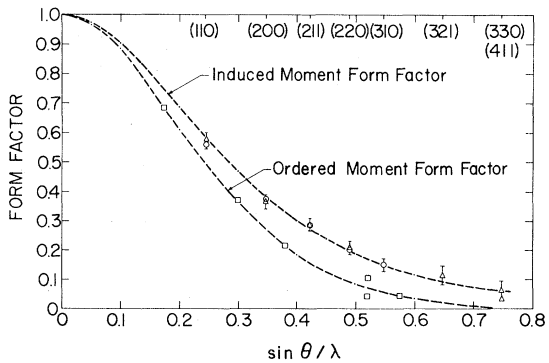

FIG. 1. Comparison of the induced-moment form factor of chromium with the magnetic form factor of the ordered state (Ref. 5). The triangles and open circles represent measurements at 27 and 100 °C, respectively.

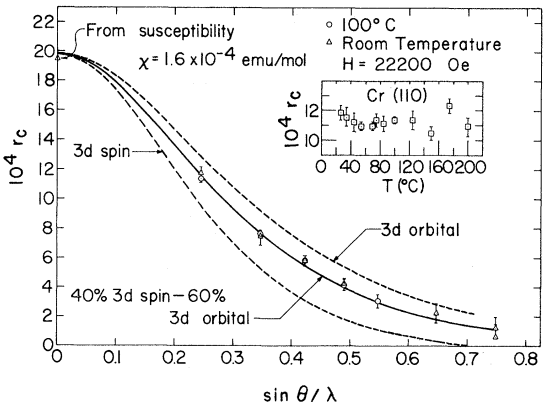

FIG. 2. Angular dependence of the induced moment magnetic scattering amplitude compared with the $3d$-spin and $3d$-orbital free-ion form factors.

This result is in disagreement with the interpretation, in terms of intrinsic localized moments, of NMR measurements[4] performed in the (40–100)°C temperature region. However, our conclusion regarding the absence of any intrinsic localized spin on the chromium atoms is consistent with paramagnetic diffuse scattering experiments,[3] which also failed to reveal the presence of any intrinsic localized moments at 210 °C. An explanation of the NMR measurements, which does not contradict the neutron diffraction results, is in terms of a spin-fluctuation model.[18]

The orbital contribution of 98×10^{-6} emu/mol obtained from our data is in good agreement with band calculations of the induced orbital paramagnetism in chromium.[19] This is of interest since the over-all bandwidth enters rather directly in the calculation. The spin contribution of 65×10^{-6} emu/mol, on the other hand, is larger by a factor of about three than various calculated values of the unenhanced spin susceptibility.[20] This seems to indicate a surprisingly large exchange enhancement, but no definite conclusions may be drawn before more detailed band calculations of the spin susceptibility become available.

V. SUMMARY

We demonstrated that the coherent magnetic scattering of neutrons by the induced moment in chromium metal may be interpreted in terms of free-ion form factors. A simple model, which assumes that the spin part of $\chi(\vec{q}, 0)$ arises from states of predominantly t_{2g} character at the Fermi surface and the orbital part from transitions between a fully occupied t_{2g} and an empty e_g energy band, is consistent with the experimental observations. The angular dependence of the coherent paramagnetic scattering amplitude is best fitted by having a 60% $3d$ orbital–40% $3d$ spin contribution to the induced moment both above and below the antiferromagnetic transition temperature. The orbital and spin susceptibilities were found to be $(98\pm3)\times10^{-6}$ emu/mol and $(65\pm2)\times10^{-6}$ emu/mol, respectively. The gyromagnetic ratio was found to be 1.25 ± 0.04. These results are consistent with measurements of the total susceptibility and gyromagnetic ratio of chromium. The magnitude of the localized induced moment has been found to be essentially temperature independent, in the (27–200)°C temperature region. Thus, we do not observe the characteristic temperature dependence expected from an intrinsic local moment on the chromium atom.

ACKNOWLEDGMENTS

The authors wish to thank F. A. Schmidt of the Ames Laboratory who kindly provided the crystals. The authors are also pleased to acknowledge helpful conversations with C. G. Shull, S. H. Liu, R. G. Barnes, and B. N. Harmon.

[1] C. G. Shull and M. K. Wilkinson, Rev. Mod. Phys. 25, 100 (1953).
[2] A. W. Overhauser, Phys. Rev. Lett. 3, 414 (1959).
[3] M. K. Wilkinson, E. O. Wollan, W. C. Koehler, and G. W. Cable, Phys. Rev. 127, 2080 (1962).
[4] R. G. Barnes and T. P. Graham, Phys. Rev. Lett. 8, 248 (1962).
[5] R. M. Moon, W. C. Koehler, and A. L. Trego, J. Appl. Phys. 37, 1036 (1966).
[6] C. Stassis, G. R. Kline, and S. K. Sinha, Phys. Rev. Lett. 31, 1498 (1973).
[7] R. Kubo and Y. Obata, J. Phys. Soc. Jpn. 11, 547 (1956).
[8] R. P. Gupta and S. K. Sinha, Phys. Rev. B 3, 2401 (1971).
[9] K. H. Oh and B. N. Harmon (private communication).
[10] C. Stassis, Phys. Rev. Lett. 24, 1415 (1970).
[11] J. Schwinger, Phys. Rev. 73, 407 (1948).
[12] O. N. Calson, F. A. Schmidt, and W. N. Paulson, Trans. ASM 57, 1 (1964).
[13] We wish to thank J. Greiner of the Ames Laboratory who kindly measured this value for our crystal.
[14] S. Asano and J. Yamashita, J. Phys. Soc. Jpn. 23, 714 (1967).
[15] See, for instance, W. Marshall and S. W. Lovesey, *Theory of Thermal Neutron Scattering* (Oxford U. P., Oxford, 1971).
[16] A. J. Freeman and R. E. Watson, Acta. Crystallogr. 14, 231 (1961).
[17] R. Huguenin, G. P. Pells and D. N. Baldock, J. Phys. F 1, 281 (1971).
[18] S. H. Liu (private communication).
[19] (a) J. S. Denbigh and W. M. Lomer, Proc. Phys. Soc. Lond. 82, 156 (1963); (b) N. Mori, J. Phys. Soc. Jpn. 20, 1383 (1965); (c) M. Shimizu (private communication); (d) K. H. Oh and B. N. Harmon (private communication).
[20] M. Shimizu, T. Takahashi, and A. Katsuki, J. Phys. Soc. Jpn. 17, 1740 (1962); R. P. Gupta and S. K. Sinha, Phys. Rev. B 3, 2401 (1971); see also, Ref. 19d.